Supplementary Information.

Building Two-Dimensional Metal-Organic Networks with Tin.

L.M. Rodríguez [a], J.D. Fuhr[a,b], P. Machaín [a], H. Ascolani* [,a],
M. Lingenfelder [c], J.E. Gayone [a,b].

S1-Experimental details.

The scanning tunneling microscopy (STM) experiments were carried on in an ultra-high vacuum system equipped with a variable-temperature STM from Omicron (model AFM/STM VT 25 DRH), a LEED optics and a homemade ion-gun for Ar^+ sputtering and also two evaporation sources, the one of Sn atoms and the one of the TCNQ molecules. The base pressure of the chamber was in the low 10^{-10} mBar range. All the reported STM images were taken at RT with the exception of the Sn/TCNQ/Cu(100) system (preparation method (ii)) which where obtained at low temperature (−143°C). Negative sample bias voltages correspond to occupied-states images. The thermal drift was compensated during the measurements by applying the facility provided by the MATRIX software used to control the STM.

In turn, the photoemission spectroscopy experiments were performed in a system for surface analysis from SPECS. The main chamber, with a base pressure in the low 10^{-10} mBar range, is equipped with a high-resolution energy analyzer, two photon sources: a monochromatized X-ray source (1486.4 eV) and a He discharge lamp (21.22 eV). In this case, the two evaporation sources were mounted in the auxiliary chamber which has a base pressure of $\sim 1 \times 10^{-8}$ mBar range. Normal emission was used for all the reported XPS spectra. In turn, emission at 10° out of normal was used for the UPS spectra; this is in order to avoid the Au(111) surface state.

The Au(111) and the Cu(100) surfaces were prepared by cycles of sputtering at 1.5 keV and annealing at ∼ 500°C. The TCNQ molecules (Sigma Aldrich, 98% purity) were used as received. The molecules were evaporated from a resistively-heated boron nitride crucible at a rate of about 0.2 monolayer (ML) per minute. We define 1 ML as the amount of molecules needed to fully cover a Au(111) surface with flat-lying adsorbed molecules. The Sn atoms (Alfa Division, 99.999% purity) were evaporated from a homemade Knudsen cell at a rate of 0.1 ML every 3 min approximately.

S2- Experimental Results: STM.

S2.1- Exploring the formation of Sn-TCNQ coordination networks on Cu(100).

We explored different preparation conditions in order to obtain metal-organic structures based on tin. To this purpose, we tried two preparation pathways (including slight variants of them): i) same as that used in the case of the Au(111) surface and ii) same as that used by Tseng *et al.* to obtain Mn-TCNQ coordination networks on the Cu(100) surface, which means evaporations of both the molecules and the Sn atoms at −123°C and then annealing at ∼ 127°C. [1] The STM images taken from the different prepared surfaces clearly show that the deposited Sn atoms do not alter the typical arrangement of the TCNQ molecules on Cu(100). Most of the Sn atoms are adsorbed on the bare Cu(100) surface forming islands (see Figures 1 and 2)

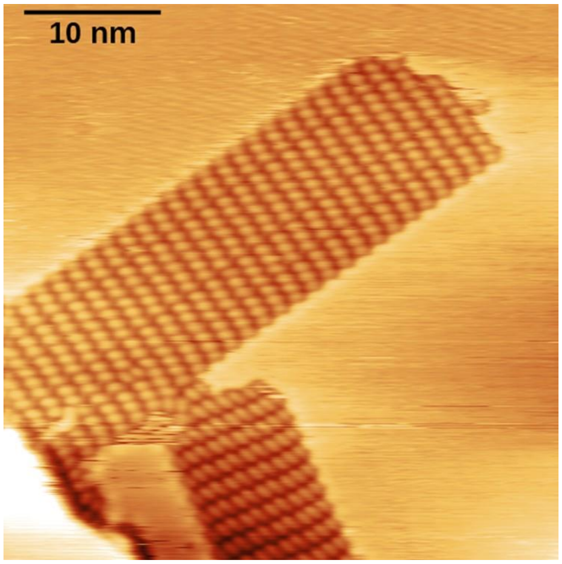

Fig. 1 STM image of TCNQ/Cu(100) measured @RT. Tunneling conditions: 2V,100pA

S2.2- Pure Sn-TCNQ/Au(111) surfaces.

In the case of the STM experiments we first adsorbed a submonolayer coverage of TCNQ on Au(111) at RT. We then adsorbed an amount of Sn atoms lower than that needed to coordinate all the adsorbed TCNQ molecules with the TCNQ/Au(111) substrate kept at ∼ 50°C. This procedure

---

[a] División Colisiones Atómicas y Física de Superficies, Centro Atómico Bariloche, CNEA and CONICET Av. E. Bustillo km 9,500, San Carlos de Bariloche, Argentina. E-mail: ascolani@cab.cnea.gov.ar
[b] Instituto Balseiro, UNCuyo. San Carlos de Bariloche, Argentina.
[c] Max Planck-EPFL Laboratory for Molecular Nanoscience, École Polytechnique Fédérale de Lausanne, Switzerland.
* Corresponding author. E-mail: ascolani@cab.cnea.gov.ar

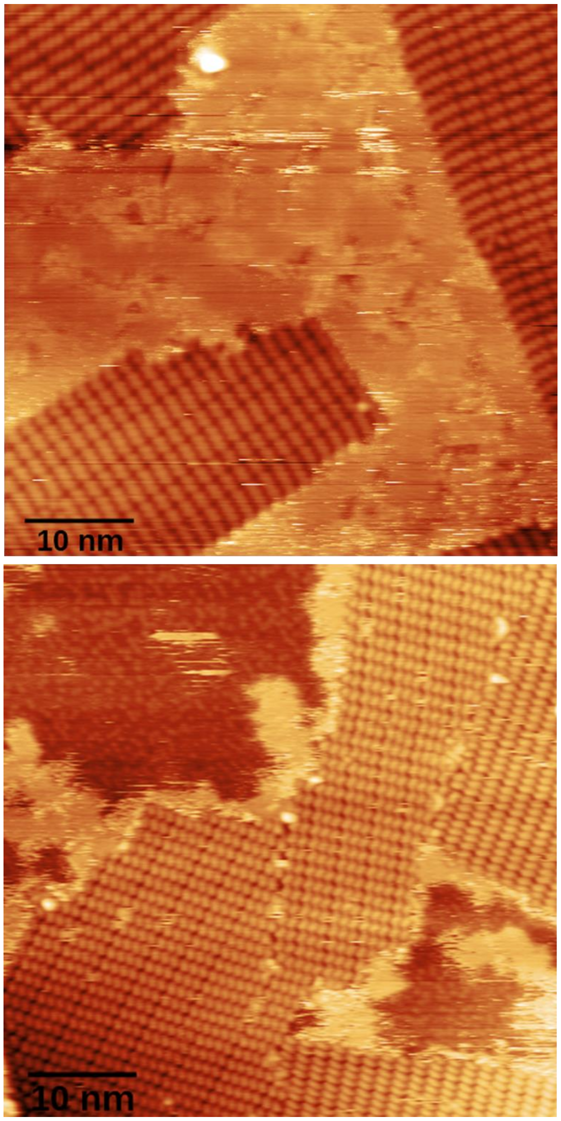

Fig. 2 (Top) STM image of the Sn/TCNQ/Cu(100) system after preparation method (i). Tunneling condition: 2.5V,100pA. (Bottom) STM image of the Sn/TCNQ/Cu(100) system after preparation method (ii) Tunneling condition: -2V,200pA.

results in an interface where the Sn:TCNQ MON coexist with the uncoordinated molecules as shown in Figure 1 of the main text. The amount of uncoordinated molecules decreases with the Sn coverage.

In order to remove the uncoordinated molecules a post-annealing is performed to 95°C. Figure 3 shows a large-scale view of a surface prepared according to this procedure. The surface is free of uncoordinated molecules. About 77% of the surface is covered by a conglomerate of relatively small domains of the Sn-TCNQ structure.

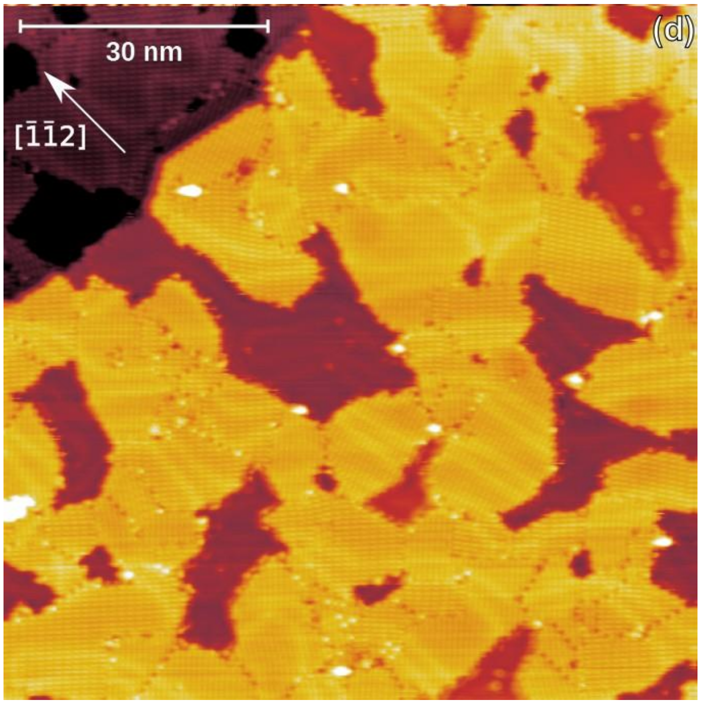

Fig. 3 STM image of the obtained Sn-TCNQ metal-organic network taken with the following conditions (2V,50pA). The high symmetry directions of the Au(111) substrate were determined from an statistical analysis of the herringbone reconstruction.

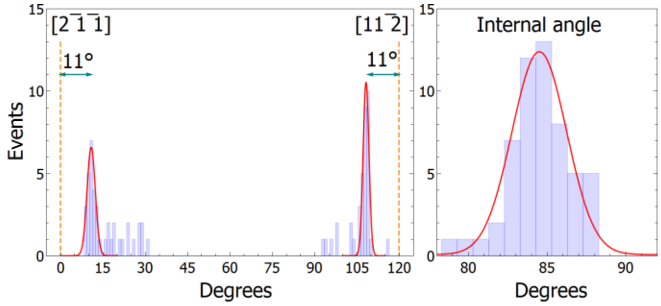

Fig. 4 Statistical analysis of the orientation and the internal unit-cell angle of the MON domains observed in Figure 3. a) : Distribution of domain orientations of the long axis of the unit cell with respect to the high-symmetry directions of the surface. b) Distribution of the internal angles of the unit cell.

To determine the orientation of the MONs domains with respect to the high-symmetry directions of the substrate and the internal angle of the unit cell, we performed a thorough statistical analysis of the orientation of the domains imaged in Figure 3. The obtained histograms are shown in Figure 4. For each domain, we determined the directions of both the long (**b**) and short (**a**) axes of the unit cell. We found that the histogram derived from the analysis of the long sides (Fig. 4(a)) has two sharp peaks located at ±11° from the indicated **[**−1−12**]** and **[**2−1−1**]** high-symmetry directions of the substrate, respectively. Thus, the great majority of domains are oriented along only 2 equivalent directions instead of the 6 that should be present in the Au(111) surface. This implies that, in the analyzed area, the orientations of the MON domains are correlated. We attribute the observed domain correlation to domain-wall interactions.

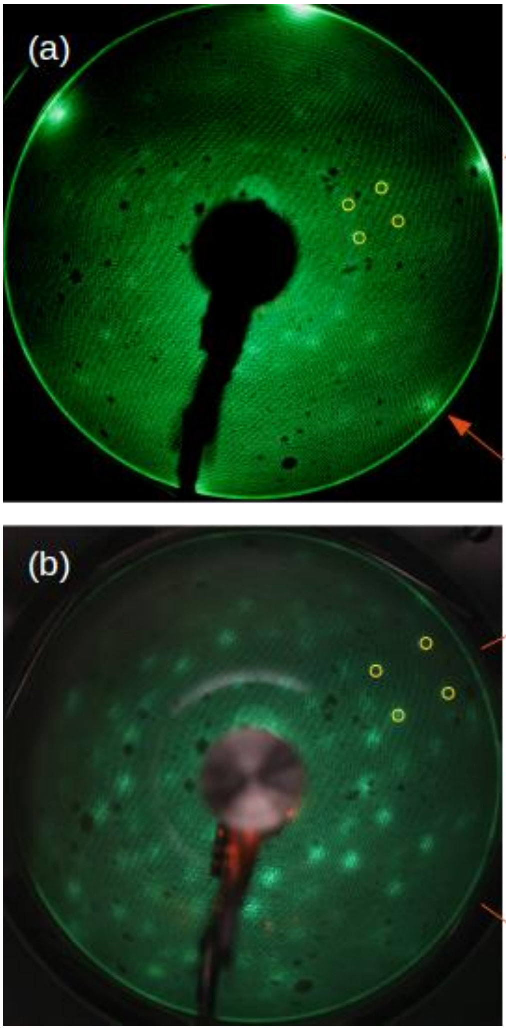

Fig. 5 LEED patterns corresponding to the Sn-TCNQ MON obtained with kinetic energies of (a):50 eV and (b):25 eV. The arrows indicate the position of the integer spots.

In order to determine the unit cell more precisely, we measured the LEED pattern from a pure Sn-TCNQ/Au(111) surface (see Figure 5) Among the most simple and commensurate unit cells that are compatible with that derived from the STM images, we have not found any one that is compatible with the experimental LEED patterns. Thus, the Sn-TCNQ network is either no-commensurate or has a very large unit cell. This is consistent with the fact that the MON overlayer is adsorbed on a reconstructed Au(111) surface.

S2.3- Thermal stability of the Sn-TCNQ/Au(111) system . Figure 6 illustrate the thermal stability **of** the Sn-TCNQ/Au(111) system. The image in panel (a) shows an STM image of the sample as prepared. Notice that the surface is free of uncoordinated molecules. The image in panel (b) was recorded after annealing the sample to 115°C during 60 minutes. After the annealing process only small islands of Sn-TCNQ MON remain on the surface. In addition, a large amount of protrusions corresponding to Sn atoms embedded in the top surface layer are clearly seen. Hence, we conclude that at 115°C a large proportion of the TCNQ molecules have desorbed from the surface due to the annealing process.

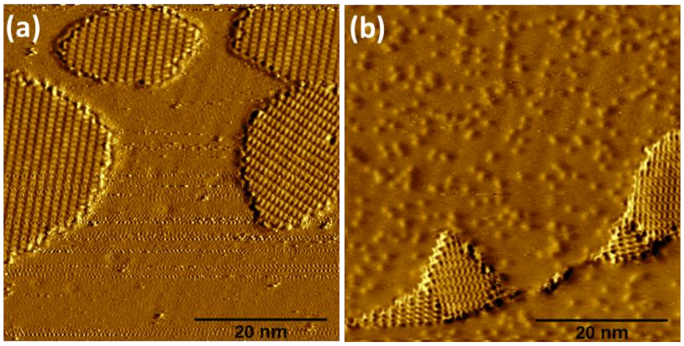

Fig. 6 STM images (gradient mode) of a pure Sn-TCNQ/Au(111) surface. (a) As prepared. (b) After annealing to 115C. The two images were measured at RT.

S3- Experimental Results: XPS.

S3.1 Preparation procedure for the Sn-TCNQ/Au(111) samples used in the photoemission experiments.

In the case of the photoemission experiments we followed 2 different preparations procedures to obtain a Sn-TCNQ MON on Au(111) with negligible uncoordinated molecules.

Procedure 1. i) The Au(111) substrate was fully covered with 1 monolayer of TCNQ molecules with the surface temperature kept at ~ 50°C. At this deposition temperature, the second molecular layer does not adsorb. ii) We then adsorbed an amount of Sn atoms lower than that needed to coordinate all the adsorbed TCNQ molecules. The surface was also at ~ 50°C during this step. In Figure 7 we show the XPS spectra corresponding to this step (top spectra in Figure7 (a), (b) and (c)). Note that the Sn3d5/2 core level presents oxidized and metallic components and the N1s core level show a shake-up satellite. iii)The third step was to desorb the uncoordinated molecules. Since in our SPECS system it was not possible to accurately set the surface temperature in the range between 95°C and 125°C (needed to desorb only the uncoordinated molecules), we applied a slow temperature ramp while monitoring the $Sn3d_{5/2}$ and N1s core levels. When the intensity of oxidized $Sn3d_{5/2}$ was at its maximum and the one of the N1s core level showed a significant drop (due to the desorption of the uncoordinated molecules) we stopped the heating procedure. In Figure 7 we also show the XPS spectra corresponding to this step (red lines). Now, the $Sn3d_{5/2}$ core level presents a single component associated to oxidized Sn, while the shake-up feature of the N1s is negligible.

Procedure 2. i) The Au(111) substrate was covered with a coverage close to one monolayer of TCNQ molecules. ii) In order to avoid the heating ramp we deposited an amount of Sn as close as possible to the amount needed to coordinate all the adsorbed TCNQ molecules with the TCNQ/Au(111) surface kept at ~ 50°C. In this case, the amount of uncoordinated molecules was considered negligible when the shake-up satellite associated to the N1s core level was not observed. We optimized the amount of deposited Sn in such a way that amount of metallic Sn atoms is low. This preparation method generates the same $Sn3d_{5/2}$, N1s and C1s core levels as those obtained with procedure 1, but with an small amount of the metallic Sn component. The data shown in figure 2 of the main text was prepared using this procedure.

In figures 2(b) and (c) of the main text the N1s and C1s spectra of a monolayer and a multilayer of TCNA/Au(111) are also shown. The monolayer was obtained following step (i) of procedure 1 mentioned above. The multilayer was obtained with the substrate kept at ~ −130°C during the TCNQ adsorption. Finally, the $Sn3d_{5/2}$ spectrum of Sn/Au(111) shown in Figure 2(a) was obtained after adsorbing Sn on the Au(111) kept at ~ 50°C (the coverage correspond to the same used for the Sn:TCNQ MON spectrum)

S3.2- Analysis of the XPS spectra.

The Binding Energy (BE) scale of the XPS spectra was calibrated by setting the BE position of the $Au4f_{7/2}$ line to 83.98 eV. The experimental N1s and C1s spectra were fitted with Voigt functions whereas the $Sn3d_{5/2}$ spectra were fitted using a Doniach-Sunjic line shape. Shirley-type backgrounds were used in every case. The C1s spectra were fitted by means of a synthesized function comprised of 4 main components with same width and with a fixed intensity ratio of 4:2:2:4 complemented with additional components to represent the minor features such as shake-up satellites and extra peaks. Table 1 summarizes the BE positions obtained from the analysis.

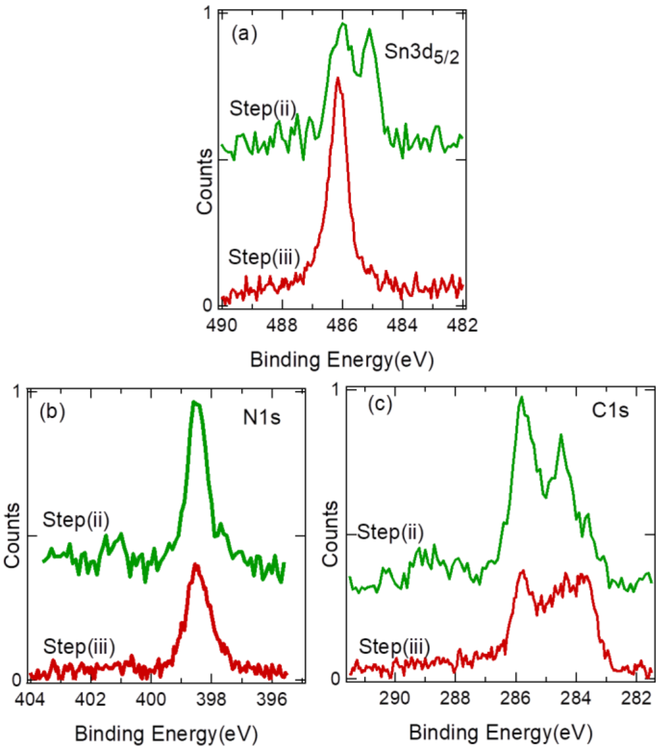

Fig. 7 $Sn3d5/2$(a),N1s(b) and C1(c) core levels for the preparation preparation procedure (1) for Sn-TCNQ/Au(111). The green and red spectra correspond to step(ii) and step(iii) respectively.

	N1s	C1s				$Sn3d_{5/2}$	
Interface		C1	C2	C3	C4	Sn2	Sn1
Sn-TCNQ MON	398.46	285.78	284.89	284.60	283.86	486.13	485.02
TCNQ Monolayer	398.61	285.98	285.76	285.37	284.58		
TCNQ Multilayer	398.95	286.35	286.08	285.69	284.88		
Sn/Au(111)							485.04

Table 1 Binding energies (expressed in eV) of the main components corresponding to the XPS spectra shown in Figure 2 of the main text.

We note that the energy separation between the components C1 and C4 increases from 1.4 to 1.92 eV (increment of 37%) when the metal-organic network is formed.

S4 - Theoretical Results

First-principles electronic structure calculations were performed within the DFT framework using the Quantum-espresso plane-wave code [2]. To take into account van der Waals interactions, we used the revised vdW-DF2 nonlocal exchanged-correlation density functional proposed by Hamada [3]. For the surface calculations we used the slab method, with four layers representing the surface and a vacuum size of ~12 Å. Except for the two lower layers that were kept fixed at the bulk distance, all the atoms in the cell were allowed to relax. Residual forces on the atoms after geometric relaxation were smaller than 10^{-3}Ry/a_0. We used ultrasoft pseudopotentials taken from Standard Solid State Pseudopotentials (SSSP) collection, [4] with an energy (density) cut-off of 55 Ry (440 Ry). Brillouin integrations were done using grids equivalent to $21 \times 21 \times 1$ for the (1×1) surface unit cell. The simulated STM images were obtained within the Tersoff-Hamann approximation.[5]

S4.1 - Structure of TCNQ on Au(111)

For comparison with the formed MON, we calculated the structural and electronic properties of a TCNQ layer on Au(111). We used a (7 -1 / 6 4) unit cell with two TCNQ molecules per cell. Figure 8 shows the obtained relaxed structured. When adsorbed on the Au(111) the TCNQ molecule remains almost flat and there are no charge transfer: a Bader atomic charge calculation gives a charge on the molecules $q < 0.06$.

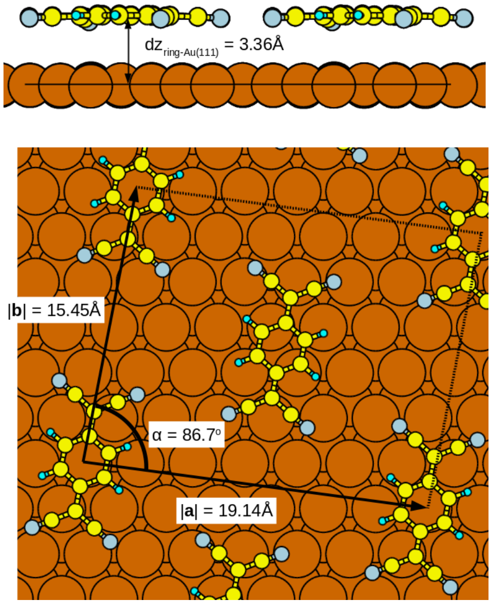

Fig. 8 Relaxed structure for a TCNQ on Au(111).

S4.2 - Structure of Sn-TCNQ: unsupported and on Au(111)

Figures 9 and 10 show the relaxed structured for a Sn-TCNQ MON on Au(111) and without substrate, respectively. A comparison of the two obtained structures indicates that they have similar features: (i) the Sn atoms and the TCNQ molecules are not in the same plane; (ii) each Sn atom is bonded to four nitrile groups in a non-symmetric arrangement: two of them at a shorter distance than the other two; (iii) the N closer to the Sn atom is higher than the N far away from the Sn. Both unit cell are also similar, although the angle is smaller for the unsupported MON.

The remarkable agreement between the Sn-N distances obtained for the Sn-TCNQ/Au(111) system with those obtained for the unsupported MON, indicates that the interaction between the Sn atoms and the nitrile groups is hardly affected by the Au(111) substrate.

The molecule-substrate interaction in the Sn-TCNQ/Au(111) system is mainly of the Van der Waals type, which is reflected in that the vertical distance between the C-ring and the top Au(111) surface layer is almost the same as that obtained for the TCNQ layer on Au(111) (Fig. 8).

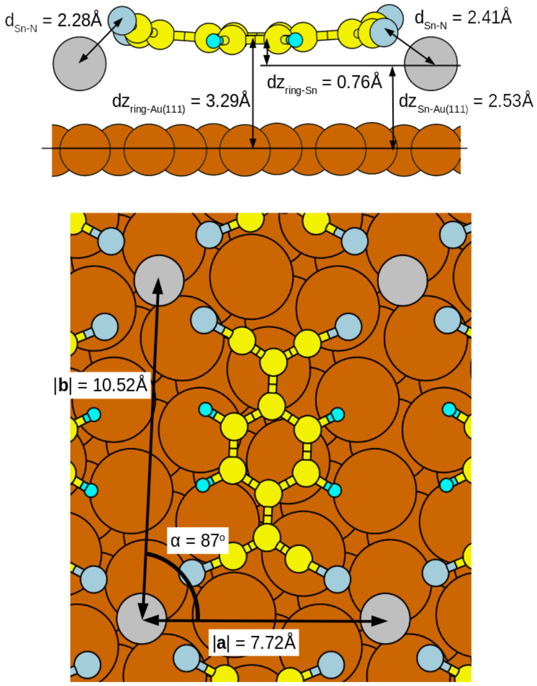

Fig. 9 Relaxed structure for a Sn-TCNQ MON on Au(111)

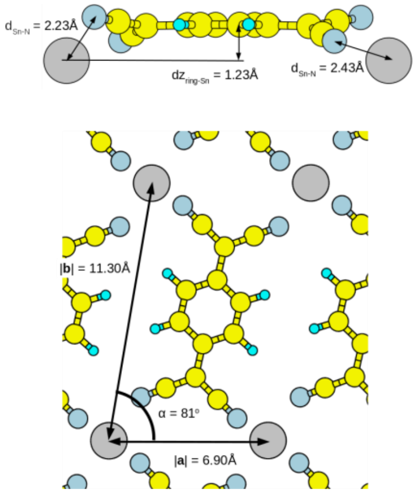

Fig. 10 Relaxed structure for an unsupported Sn-TCNQ MON.

S4.3 - Simulated STM Images

Figure 11 compares the empty- and filled-states STM images theoretically simulated for the Sn-TCNQ/Au(111) system. The red circles superimposed to these images are centred at the position of the Sn atoms and delimit the region of the Sn-N bonds. We note that in the red circle there are four bright spots, two of them more intense than the other two. Clearly, the observed asymmetry and the position of the spots indicates that they are mainly related to the four nitrile groups coordinating the central Sn atom. The Sn atoms are not "seen" in the images likely due to the fact they are located at a lower vertical position than the molecular C-ring.

Comparing the two images, it can be seen that the mean intensity in the region of the Sn-N bonds (red circle) relative to the mean intensity in the region of the molecular C-ring (blue circle), is higher in the filled-state image. Hence, the simulated images qualitatively reproduce the changes in brightness observed in the experimental images when the bias polarity is inverted.

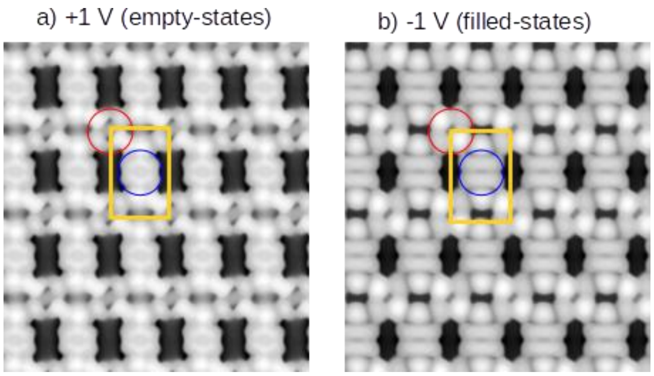

Fig. 11 Simulated STM Images for the Sn-TCNQ/Au(111) system. a) Empty-state image at +1 eV. b) Filled-state image at -1 eV. The unit cell is indicated in the two cases (yellow rectangles). Additionally, the positions of the Sn atoms are indicated with red circles that also contain the associated four nitrile ligands. The blue circle indicates the region of the molecular C-ring.

S4.4 - Simulation of the C1s and N1s photoemission spectra

As the DFT where performed using a pseudopotential method, the core electrons are not explicitly included in a self-consistent field (SCF) calculation. We then obtained the C(1s) chemical shifts by total energy differences between "standard" and "core-hole" calculations. [6,7] To evaluate the relative binding energy of a given atom we used a different "excited-state" pseudopotential for this atom which has a core hole and an extra valence electron.

The absolute value of the binding energy (BE) is not well described by this method. The reason for this is that the Fermi energy is not defined accurately enough in the simulated systems due to the small number of layers used to describe the substrate. This means that it is not possible, within our theoretical approach, to compare the BE positions of the N1s and C1s core levels corresponding to the Sn-TCNQ/Au(111) system with those of the TCNQ/Au(111). Thus, we only discuss the differences between the BEs of the inequivalent atoms within each structure. To simulate C1s spectra we then take BE=0 for the C atoms in the nitrile groups, and we use gaussian distributions (with a width of 0.2eV) centered at each calculated relative BE.

Figure 12(a) shows the simulated C-1s photoemission spectra for a monolayer of TCNQ adsorbed on Au(111) and a Sn-TCNQ MON on Au(111) respectively. The total spectra is decomposed in the contribution of each inequivalent type of C atom **(see Figure 12c).** When the MON is formed, the main effect is a appreciable shifted of the BE corresponding to the C-ring with respect to the other C atoms, resulting in a width increment of 33%.

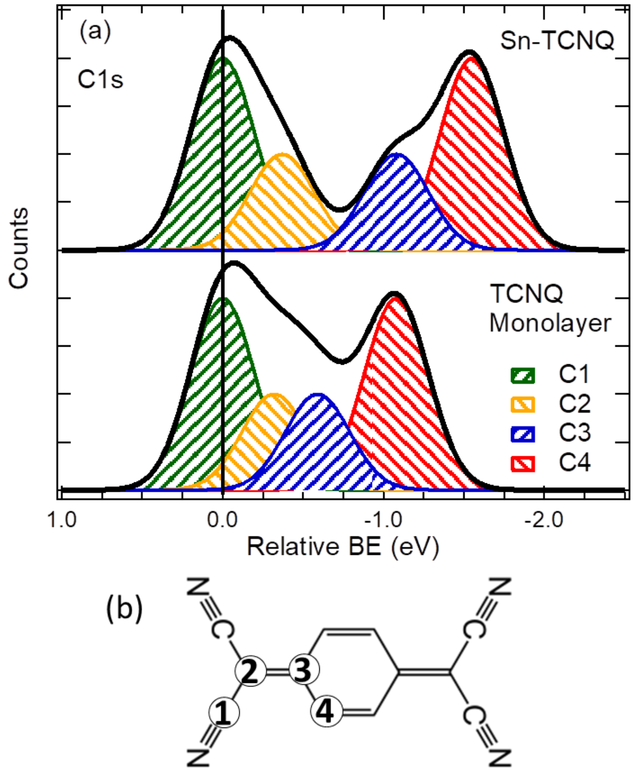

Fig. 12 (a) Simulated C1s photoemission signal: Monolayer of TCNQ adsorbed on Au(111) (bottom) and Sn-TCNQ coordination network adsorbed on Au(111) (top). (b): Scheme of the TCNQ molecule where the 4 inequivalent C atoms are indicated.

References

1 T.-C. Tseng, C. Lin, X. Shi, S. Tait, X. Liu, U. Starke, N. Lin, R. Zhang, C. Minot, M. A. V. Hove, J. Cerdá and K. Kern, *Phys. Rev. B*, 2009, **80**, 155458.

2 P. Giannozzi, S. Baroni, N. Bonini, M. Calandra, R. Car, C. Cavazzoni, D. Ceresoli, G. L. Chiarotti, M. Cococcioni and I. Dabo, *J. Phys.: Condens. Matter*, 2009, **21**, 395502.

3 Hamada and Ikutaro, *Phys. Rev. B*, 2014, **89**, 121103.

4 *Materials Cloud Standard Solid State Pseudopotentials (SSSP)*, https://www.materialscloud.org/discover/sssp/table/efficiency.

5 J. Tersoff and D. R. Hamann, *Phys. Rev. B*, 1985, **31**, 805–813.

6E. Pehlke and M. Scheffler, *Phys. Rev. Lett.*, 1993, **71**, 2338–2341.

7L. Bianchettin, A. Baraldi, S. de Gironcoli, S. Lizzit, L. Petaccia, E. Vesselli, G. Comelli and R. Rosei, *Phys. Rev. B*, 2006, **74**, 045430.